Discrete Ginzburg-Landau solitons

Nikolaos K. Efremidis and Demetrios N. Christodoulides
School of Optics/CREOL, University of Central Florida, Orlando, Florida 32816-2700
(Received 2 August 2002; published 12 February 2003)

We demonstrate that discrete solitons are possible in Ginzburg-Landau lattices. As a result of discreteness, we find that this system exhibits a host of features that have no counterpart whatsoever in either the continuous limit or in other conservative discrete models.

DOI: 10.1103/PhysRevE.67.026606 PACS number(s): 42.65.Tg, 05.45.Yv

The complex Ginzburg-Landau (GL) equation is known to play a ubiquitous role in science. This equation is encountered in several diverse branches of physics, such as, for example, in superconductivity and superfluidity, nonequilibrium fluid dynamics and chemical systems, nonlinear optics, Bose-Einstein condensates, and in quantum field theories [1–5]. In general, the very nature of the GL system is such that can lead to extraordinary rich behavior ranging from chaos and pattern formation to self-localized solutions or solitons. In the latter regime, GL dissipative solitons (or autosolitons) are possible as a result of the interplay between linear and nonlinear gain, nonlinearity, and complex dispersion [6–9]. Over the years, the soliton solutions of the Ginzburg-Landau equation and their underlying dynamics have been the subject of intense investigation. Such pulselike soliton states were first identified with in the context of the cubic GL model [6,7] and subsequently in the generalized quintic regime [4,8,9] and, typically, they represent chirped coherent structures (or one-dimensional defects) that are obtained through heteroclinic trajectories in the phase space of the stationary GL equation. Several types of solitary wave solutions of the continuous GL equation have been identified over the last years. These include flat-top solutions in one and two dimensions [10,11], erupting and creeping solitons [11,12], and spiraling solitons carrying topological charge [13,14].

In addition to the well-studied continuous GL equation, discrete Ginzburg-Landau (DGL) models have also been considered in the literature [15–18]. These DGL lattices are quite often used to describe a number of physical systems such as Taylor and frustrated vortices in hydrodynamics [15] and semiconductor laser arrays in optics [16,17]. In these latter studies, the DGL model has been predominantly used in connection with spatio-temporal chaos, instabilities, and turbulence [18]. Nevertheless, in spite of previous research activity, no coherent structures such as self-localized solutions or solitons have been identified in the DGL system. It is therefore natural for someone to ask whether such discrete Ginzburg-Landau or DGL solitons indeed exist. And, if that is the case, what are their underlying properties and how do they differ from their continuous counterparts?

In this paper, we demonstrate that discrete solitons (DS) are possible in Ginzburg-Landau lattices. More specifically, we show that this system exhibits unique complex dispersion properties associated with a Brillouin zone. As a result, the discrete dispersion (diffraction) behavior of a GL lattice differs substantially from that encountered in conservative arrays [19,20]. In general, two new types of DGL solitons can exist under the same conditions. These solutions are located either at the base or at the edge of the Brillouin zone and bifurcate at different values of the linear gain. As a result of discreteness, we find that this system exhibits features that have no counterpart whatsoever in either the continuous GL limit or in other conservative discrete models [19,20] [as in discrete nonlinear Schrödinger (DNLS) chains]. These include, for example, on-site and intrasite bright DGL solitons that can both be stable as well as new bifurcation types that cannot be identified in the continuous case.

In general, the cubic-quintic DGL equation is given by

$$i\dot{u}_n - i\epsilon u_n + \alpha(u_{n+1}+u_{n-1}) + p|u_n|^2 u_n + q|u_n|^4 u_n = 0, \tag{1}$$

where $p=p_r+ip_i$, $q=q_r+iq_i$, $\alpha=\alpha_r+i\alpha_i$, ϵ is a real parameter, and $\dot{u}_n = du_n/dz$. Physically, the discretization in Eq. (1) occurs by applying the tight binding approximation (or coupled mode theory) [17,21]. The original, periodic in space, continuous system is expanded in local modes, whose amplitudes are described by the corresponding discrete model. In Eq. (1) α_r accounts for the energy tunneling between adjacent elements of the lattice, while its imaginary part stands for gain (losses) due to coupling. The real parts of p and q represent the strength of the cubic and quintic nonlinearity of the system, while ϵ, p_i, q_i are the linear and nonlinear gain (loss) coefficients.

Within the context of nonlinear optics, the DGL equation arises in the description of semiconductor laser arrays [17], where the quintic term can account for the gain and nonlinearity saturation of the lasing medium. The DGL equation can also describe the dynamics of an open Bose-Einstein condensate. In this case, the lattice potential is created by the interference of two optical standing waves [22] and, thus, solitons of the discrete nonlinear Schrödinger type are known to exist [23]. The dissipation of the Bose-Einstein condensate naturally occurs in an open condensate while gain can result from the interaction between the condensed and the uncondensed atoms [24,25]. Notice, than in all of these cases, it is a common practice to write the original saturable nonlinearity of the system in terms of a cubic-quintic expansion that, in turn, conveys the fundamental properties of the original model [17,25].

We begin our analysis by considering the linear dispersion properties of the DGL equation. To do so, we write $u_n \propto \exp(ikz - i\theta n)$, where $k=k_r+ik_i$ is the complex propaga-

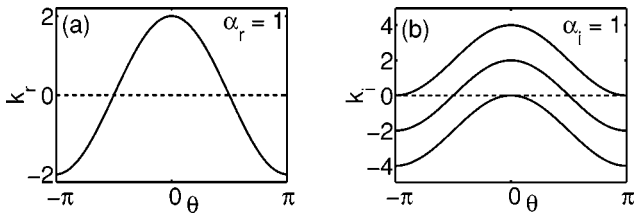

FIG. 1. (a) The dispersion curve of the array when $\alpha_r=1$ and (b) k_i (associated with the instability growth rate) as a function of θ for $\alpha_i=1$ and $\epsilon=-2,0,2$.

tion wave number and θ is the wave momentum inside the lattice. The real and imaginary parts of Eq. (1) are then found to satisfy

$$k_r=2\alpha_r\cos\theta, \quad k_i=-\epsilon+2\alpha_i\cos\theta. \tag{2}$$

In Fig. 1, k_r and k_i are depicted as a function of θ. Equation (2) describes the dispersive properties of the lattice within the Brillouin zone as defined in the region $|\theta|\leqslant\pi$. When $|\theta|<\pi/2$ and $\alpha_r>0$, the curvature of the dispersion relation [Eq. (2)] implies that the effective diffraction of the array is normal. On the other hand, when $\pi/2<|\theta|<\pi$ (and $\alpha_r>0$) the effective diffraction of the array becomes anomalous and of course these regimes are reversed for $\alpha_r<0$.

The imaginary part of the propagation wave number [Eq. (2)], is directly related with the growth rate of the perturbations of the zero solution. In particular, any perturbation frequency θ that satisfies the condition $k_i<0$, will grow exponentially with a growth rate $g_d(\theta)=\epsilon-2\alpha_i\cos\theta$. We emphasize that this growth rate is a periodic function of θ with period 2π, i.e., $g_d(\theta+2\pi n)=g_d(\theta)$, where n is an integer. From all the possible frequencies θ within the Brillouin zone, only those that satisfy the inequality $\epsilon>2\alpha_i\cos\theta$ will eventually develop instabilities. Therefore, the zero solution is absolutely stable for $\epsilon<-2|\alpha_i|$. On the other hand, when $\epsilon>2|\alpha_i|$ every frequency is amplified, and the maximum growth rate (that occurs either at the base or at the edge of the Brillouin zone) is given by $\epsilon+2|\alpha_i|$. In the regime between the two aforementioned cases, i.e., when $-2|\alpha_i|<\epsilon<2|\alpha_i|$, only a subset of the frequencies (those satisfying $\epsilon>2\alpha_i\cos\theta$) will be amplified while the rest of them will decay. Note that the instability behavior of the zero solution of the DGL is fundamentally different from that arising in the continuous GL limit where it is described by $g_c(\theta)=\epsilon'+\alpha_i\theta^2$ [26]. Apparently, in the continuous limit, the stability properties are strongly affected by the sign of the ''diffusion'' term, α_i, i.e., for $\alpha_i>0$ the zero solution will always be unstable, regardless of the value of ϵ. Thus, in order to stabilize the background of a self-localized state, it is essential to have $\alpha_i<0$. On the other hand, the DGL model has the interesting property that the background can be stabilized for both signs of α_i by appropriately choosing the linear gain ϵ of the system. We would like to mention that, in the linear regime, Eq. (1) can be solved analytically. When only one lattice element is initially excited (say $n=0$ at $z=0$), the field profile at z is given by

$$u_n(z)=u_0J_n(2\alpha z)e^{i\pi n/2}e^{\epsilon z}, \tag{3}$$

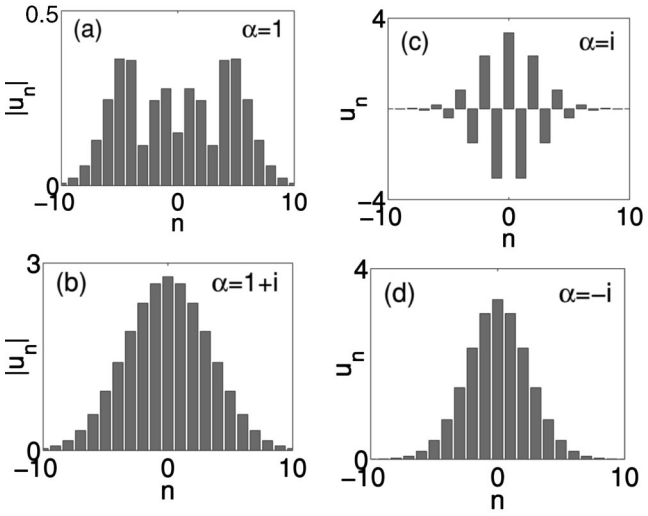

FIG. 2. Field profile of a linear impulse response of the lattice at $z=3$. In (a) $\epsilon=0$, while in (b)–(d) $\epsilon=-1$.

where $J_n(x)$ (with complex argument) is a Bessel function of the first kind and of integer order n. The evolution of more involved initial field patterns can be readily obtained by simple superposition of this impulse response. In Figs. 2(a)–2(d) the impulse response of the lattice at $z=3$ is depicted for $\alpha=1,\ 1+i,\ i,\ -i$, respectively. In Fig. 2(c) the out-of-phase mode is preferentially amplified, while in Fig. 2(d) the mode is in phase at the output.

We will now investigate the structure as well as some of the basic properties of DS states existing in the GL lattice. To do so, we look for stationary localized modes $u_n=\exp(i\lambda z)v_n$ of Eq. (1) and the resulting algebraic system is solved numerically using the Newton iteration method. Note that Eq. (1) is subject to certain symmetries that can be used to reduce the parameter space of the system in study. We notice that, by employing the phase transformation $u_n\rightarrow u_n\exp(i\pi n)$ along with $\alpha\rightarrow-\alpha$, Eq. (1) remains invariant. This, in turn, allows the one-to-one mapping $\alpha\leftrightarrow-\alpha$. Here, without any loss of generality, we assume that $\alpha_r>0$. A second symmetry also exists, i.e., $z\rightarrow-z$, and $u_n\rightarrow\exp(i\pi n)u_n$, $p\rightarrow-p$, $q\rightarrow-q$, which is used by applying the additional constraint $p_r>0$ to the system. In doing so, we consider immobile GL discrete solitons that reside either at the base ($\theta=0$), or at the edge ($\theta=\pi$) of the Brillouin zone [27]. For $\theta=0$, the DS bifurcates from the zero solution at $\epsilon=2\alpha_i$, while in the case $\theta=\pi$ the DS bifurcates at $\epsilon=-2\alpha_i$. It is important to note that the existence of these two bifurcation points is a result of the periodicity introduced by the lattice model and is in clear contradistinction to the continuous GL equation, where only one bifurcation occurs when the linear gain is zero. The connection between the DS states and the solitons of the continuous GL equation is established for broad enough solutions. In this regime one can apply a Taylor series expansion and, as a result, Eq. (1) can be approximated by the continuous GL equation (see Ref. [26]). Then, in the linear case, the periodic diffraction relation of the discrete model can be approximated by a parabolic in the continuous case. Close to the bifurcation points

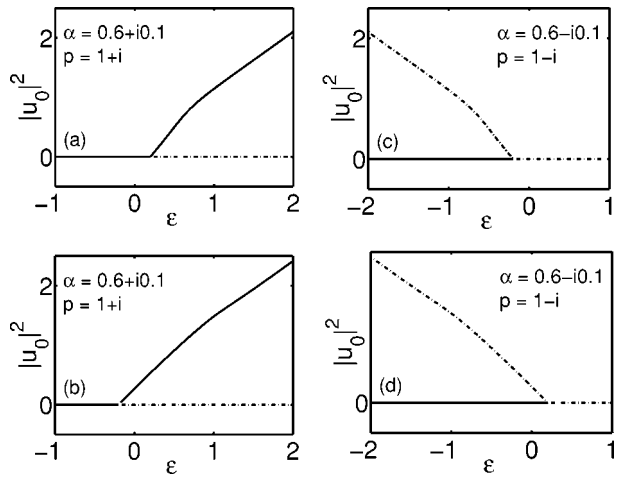

FIG. 3. Typical codimension one bifurcation diagrams of the cubic DGL model. In all bifurcation figures, solid and dash-dotted curves represent stable and unstable branches, respectively.

the solutions become very broad and, therefore, can be approximated by the soliton states of the continuous GL equation [6,9,26]. For example, for the continuous cubic GL system (see Ref. [26]) the maximum intensity of a broad discrete soliton is related to ϵ' in a linear fashion

$$u_0^2=\frac{-3\mu(\alpha_r^2+\alpha_i^2)\epsilon'}{a[2\mu\alpha_r+\alpha_i(1-\mu^2)]}, \tag{4}$$

where $\mu=(3b\pm\sqrt{9b^2+8a^2})/2a$, $a=p_r\alpha_i-p_i\alpha_r$, $b=p_r\alpha_r-p_i\alpha_i$. On the other hand, when the solution is highly confined inside the lattice ($|u_{\pm1}|/|u_0|\ll1$), one can accurately estimate its maximum amplitude to be

$$u_0^2=\left(\sqrt{\frac{\epsilon}{p_i}}-\sqrt{\frac{p_i}{\epsilon}}\frac{2p_r\alpha_r\alpha_i+p_i(\alpha_i^2-\alpha_r^2)}{\epsilon(p_r^2+p_i^2)}\right)^2, \tag{5}$$

while similar expressions are obtained for the soliton propagation number λ as well as for $u_{\pm1}$ for both the cubic and the quintic models. Again, for asymptotically large values of the maximum intensity, $|u_0|^2$ is linearly related to ϵ. In general, these highly confined modes are accurately described by

$$u=u_0\exp(-s|n|+i\lambda z), \tag{6}$$

where the parameters of the solution satisfy $\lambda+i\epsilon=2\alpha\cosh s$ and $\sinh s=u_0^2(p+qu_0^2)/(2\alpha)$. In addition, one can

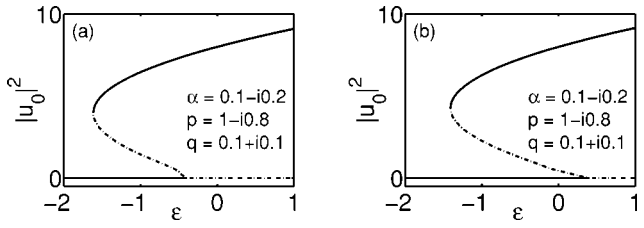

FIG. 4. (a) A highly confined DS solution in the normal diffraction regime and (b) the corresponding DS that resides at the edge of the Brillouin zone, when $\alpha=0.1-0.2i$, $p=1-i0.8$, $q=0.1+0.1i$, $u_0=2.1$.

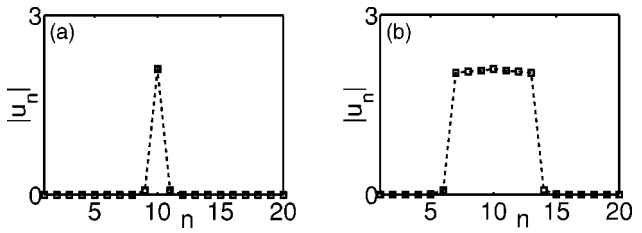

FIG. 5. Bifurcation diagrams of the quintic DGL equation (a) at the base and (b) at the edge of the Brillouin zone.

obtain valuable information from the DS tails since locally $u_n\propto\exp(i\lambda z-s|n|)$ is satified. In this case, the relations (constraints) $\lambda=2[\alpha_r\cosh(s_r)\cos(s_i)-\alpha_i\sinh(s_r)\sin(s_i)]$ and $\epsilon=2[\alpha_r\sinh(s_r)\sin(s_i)+\alpha_i\cosh(s_r)\cos(s_i)]$ hold true.

In Fig. 3, typical codimension one bifurcation diagrams of the cubic DGL model are depicted. Figures 3(a) and 3(c) show bifurcations for DS located at the base of the Brillouin zone whereas the curves of Fig. 3(b) and (d) correspond to the edge of the zone. As in the continuous GL case, these bifurcations are supercritical when $p_i>0$ and subcritical when $p_i<0$. In all bifurcation figures, solid and dash-dotted curves represent stable and unstable branches, respectively.

Close to the bifurcation point, the DS are quite broad, and, as a result, the numerically found curves shown in Fig. 3 (with either $\theta=0$ or $\theta=\pi$) are well approximated by Eq. (4). Also, when the maximum intensity becomes relatively high, the solutions residing in the normal diffraction regime become highly localized inside the lattice. Fig. 4(a) depicts such a highly confined DS (at the base of the Brillouin zone), which is in excellent agreement with the analytical results of Eq. (6). On the other hand, in the anomalous discrete diffraction regime (at the edge of the Brillouin zone), a rather peculiar feature arises; the amplitude profile becomes broader and flatter with stronger chirp. We attribute this property to the rather involved energy flow within the GL DS under anomalous diffraction conditions. As an example, Fig. 4(b) shows the field of a high-intensity DS in the anomalous diffraction regime that extends over seven lattice points. Similar types of solutions (flat top) can also be found in the continuous Ginzburg-Landau model [10,11]. On the other hand, these discrete flat-top solutions exist when the maximum intensity of the solutions is above a certain threshold, and their stability properties may be relevant to the modulational instability of the corresponding continuous-wave solution. However, the possible bifurcation of these solutions is an issue that merits further investigation.

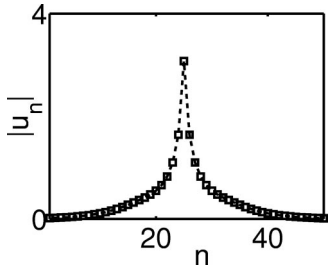

FIG. 6. A cusplike DS solution for $\alpha=0.4-2i$, $p=0.1-0.4i$, $q=0.43i$ and $\epsilon=-0.4$.

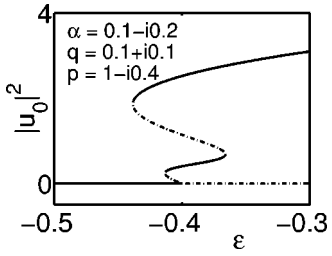

FIG. 7. A subcritical bifurcation followed by three successive saddle-node bifurcations at $\theta=0$.

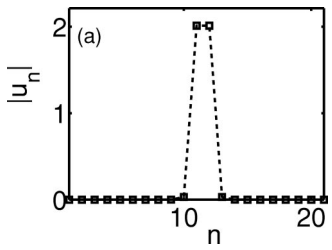

FIG. 8. In-phase stable intrasite DS for $\alpha=0.1-i0.1$, $p=0.2-i6$, $q=0.2+i$, and $\epsilon=-8$.

In general, the stability properties of the cubic DGL solitons can be identified from the corresponding bifurcation diagrams. A subcritical DS will be unstable, whereas an unstable background can destabilize a supercritical DS. The properties of the bifurcation diagrams can be modified when the quintic term in Eq. (1) is nonzero. In fact, a saddle-node bifurcation emerges if the condition $p_i q_i<0$ is satisfied. It is then of interest to determine the parameter space where absolutely stable DS exist. To realize this, it is necessary that the zero background on which these discrete modes reside is stable for any perturbation frequency, i.e., $\epsilon<-2|\alpha_i|$. By taking this into account and knowing from standard bifurcation theorems that stable and unstable manifolds alternate, one can then conclude that necessary conditions for DS stability are $p_i<0$ and $q_i>0$. In Fig. 5 such bifurcation diagrams of the quintic model satisfying the necessary stability conditions are depicted. The curves shown in Figs. 5(a) and 5(b) correspond to the base and the edge of the Brillouin zone, respectively. The stability of these solutions was then investigated by performing numerical simulations. The DS shown in Fig. 4(a) lies on the upper branch of the bifurcation diagram and was also verified numerically to be stable. On the other hand, the solution shown in Fig. 4(b) happens to be unstable.

We would also like to mention that in certain range of parameters the DS solutions of the DGL equation can exhibit interesting behavior; the tails of the DS become very broad (occupying many lattice sites), whereas the central part of it is confined and displays a cusplike feature as shown in Fig. 6. Note that no such cusp soliton structures are possible in either the continuous GL regime or in DNLS lattices. To understand this behavior one may use the relation $\lambda+i\epsilon=2\alpha\cosh s$, from where the rate of decay, s_r, of the soliton tails in Eq. (6) can be determined. In the case of Fig. 6, $s_r=0.2$ which indeed justifies the slow field decay at the tails.

More complicated bifurcation diagrams that have no analog in the continuous GL case also appear in the discrete model. For example, in Fig. 7 (normal diffraction regime) we can observe a subcritical bifurcation that is followed from three successive saddle-node bifurcations. As a result, four different branches of nonzero solutions exist allowing up to two stable DS for the same value of ϵ.

Except from the DS that are centered on a single lattice point (on site), two different types of DS that are centered between two lattice points (intrasite) exist. These are characterized by the phase difference between the two central lattice points that can be either 0 or π when the solutions are highly confined. In the DNLS regime, the π-out-of-phase intrasite DS are known to be stable [28] for relatively strong nonlinearities, whereas, the in-phase intrasite DS are always unstable because of oscillatory instabilities. Yet, in the DGL lattice system, we have identified regimes where both types of DS solutions are stable. In Fig. 8 such a stable intrasite in-phase state is depicted. For these values of the parameters both the in-phase and the out-of-phase DS are stable. Their intensity profiles are almost identical, and their main difference is in the relative phase between the high-intensity lattice sites, which is 0 or π. The stability of these DS was checked dynamically against symmetry breaking perturbations. A more detailed stability analysis of these DS will be presented elsewhere.

In conclusion, we have demonstrated that discrete solitons are possible in Ginzburg-Landau lattices. As a result of discreteness, this system exhibits several features that have no counterpart whatsoever in either the continuous limit or in other conservative discrete models. Before closing, we would like to mention that there are still several issues that may merit further investigation. These include, for example, the existence of other DGL coherent structures, such as, fronts, sources, as well as sinks. Finally, we mention that it may also be of interest to investigate the effect of higher-order discrete diffraction effects that can appear, for example, in a discretized version of the complex Swift-Hohenberg equation. Physically, this is possible by using the zigzag configuration suggested in Ref. [29].

This work was supported by an ARO MURI and by the Pittsburgh Supercomputer Center.

[1] M.C. Cross and P.C. Hohenberg, Rev. Mod. Phys. **65**, 851 (1993).

[2] Y. Kuramoto, *Chemical Oscillations, Waves and Turbulence* (Springer, Berlin, 1984).

[3] I.S. Aranson and L. Kramer, Rev. Mod. Phys. **74**, 99 (2002).

[4] N.N. Akhmediev and A. Ankiewicz, *Solitons, Nonlinear Pulses and Beams* (Chapman and Hall, London, 1997).

[5] P. Manneville, *Dissipative Structures and Weak Turbulence* (Academic, San Diego, 1990).

[6] L.M. Hocking and K. Stewartson, Proc. R. Soc. London, Ser. A

326, 289 (1972); N.R. Pereira and L. Stenflo, Phys. Fluids **20**, 1733 (1977).
[7] K. Nozaki and N. Bekki, J. Phys. Soc. Jpn. **53**, 1581 (1984).
[8] W. van Saarloos and P.C. Hohenberg, Physica D **56**, 303 (1992).
[9] R. Conte and M. Musette, Physica D **69**, 1 (1993); P. Marcq, H. Chaté, and R. Conte, *ibid.* **73**, 305 (1994).
[10] N.N. Akhmediev, V.V. Afanasjev, and J.M. Soto Crespo, Phys. Rev. E **53**, 1190 (1996).
[11] L.C. Crasovan, B.A. Malomed, and D. Mihalache, Phys. Lett. A **289**, 59 (2001).
[12] J.M. Soto-Crespo, N. Akhmediev, and A. Ankiewicz, Phys. Rev. Lett. **85**, 2937 (2000).
[13] P.S. Hagan, SIAM (Soc. Ind. Appl. Math.) J. Appl. Math. **42**, 762 (1982).
[14] L.C. Crasovan, B.A. Malomed, and D. Mihalache, Phys. Rev. E **63**, 016605 (2001).
[15] H. Willaime, O. Cardoso, and P. Tabeling, Phys. Rev. Lett. **67**, 3247 (1991).
[16] S.S. Wang and H.G. Winful, Appl. Phys. Lett. **52**, 1774 (1988); H.G. Winful and S.S. Wang, *ibid.* **53**, 1894 (1988).
[17] K. Otsuka, *Nonlinear Dynamics in Optical Complex Systems* (KTK Scientific Publishers, Tokyo, 1999).
[18] K. Otsuka, Phys. Rev. Lett. **65**, 329 (1990); H.G. Winful and L. Rahman, *ibid.* **65**, 1575 (1990).
[19] D.N. Christodoulides and R.I. Joseph, Opt. Lett. **13**, 794 (1988).
[20] H.S. Eisenberg, Y. Silberberg, R. Morandotti, A.R. Boyd, and J.S. Aitchison, Phys. Rev. Lett. **81**, 3383 (1998).
[21] C. Kittel, *Introduction to Solid State Physics* (Wiley, New York, 1986).
[22] B.P. Anderson and M.A. Kasevich, Science **282**, 1686 (1998).
[23] A. Trombettoni and A. Smerzi, Phys. Rev. Lett. **86**, 2353 (2001).
[24] B. Kneer, T. Wong, K. Vogel, W.P. Schleich, and D.F. Walls, Phys. Rev. A **58**, 4841 (1998).
[25] F.T. Arecchi, J. Bragard, and L.M. Castellano, in *Bose-Einstein Condensates and Atom Lasers*, edited by S. Martellucci, A.N. Chester, A. Aspect, and M. Inguscio (Kluwer, New York, 2002).
[26] It is often useful to consider Eq. (1) in the so-called continuous limit at the base (edge) of the Brillouin zone, where it can be approximately written as $iU_z - i\epsilon' U \pm \alpha U_{xx} + p|U|^2 U + q|U|^4 U = 0$, where $\epsilon' = \epsilon \mp 2\alpha_i$, respectively.
[27] Y.S. Kivshar, Opt. Lett. **18**, 1147 (1993).
[28] S. Darmanyan, A. Kobyakov, and F. Lederer, Zh. Éksp. Teor. Fiz. **113**, 1253 1998 [Sov. Phys. JETP **86**, 682 (1998)]; P.G. Kevrekidis, A.R. Bishop, and K.O. Rasmussen, Phys. Rev. E **63**, 036603 (2001).
[29] N.K. Efremidis and D.N. Christodoulides, Phys. Rev. E **65**, 056607 (2002).